

Efficiency Enhancement of Perovskite Solar Cells Based on Graphene Nanocomposites as Electrons and Holes Transport Layers

Hayder Hasan Ali*

Department of Science, College of Basic Education, University of Sumer – Iraq

Article information

Article history:

Received: October, 06, 2023

Accepted: November, 05, 2023

Available online: December, 14, 2023

Keywords:

Perovskite,
CsPbBr₃ QDs,
Nanocomposites

*Corresponding Author:

Hayder Hasan Ali
hdown1992@gmail.com

DOI:

<https://doi.org/10.53523/ijoirVol10I3ID372>

This article is licensed under:

[Creative Commons Attribution 4.0 International License](https://creativecommons.org/licenses/by/4.0/).

Abstract

This study investigates the use of TiO₂/G and ZrO₂/G transport layers in perovskite solar cells. The hydrothermal technique was used to synthesize the transport layers. According to the results, using TiO₂/G as an electron transport layer enhances the transfer of negative charges from perovskites, which increases the efficiency of the solar cell. This is thanks to improved electrical conductivity and less loss of negative charges in the transport layer. The positive gap transition from the perovskite layer to the gap transport layer was enhanced using ZrO₂/G. The chemical and physical properties of ZrO₂/G help to build a strong interface with perovskite, which promotes gap crossing and reduces the loss of positive charges. Regarding the photonic layer, the efficiency of the solar cell increased significantly when CsPbBr₃ quantum dots were used as the active element due to their strong abilities to absorb light from the visible light spectrum according to absorption spectrometry measurements. The efficiency of converting light into electrical charges increases because they can absorb more sunlight, including low-level solar energy. Quantum dots have efficient charge transfer paths, which reduces charge loss and improves conversion efficiency. CsPbBr₃ quantum dots are chemically and crystalline stable. These factors work together to increase the efficiency of the perovskite solar cell when using CsPbBr₃ quantum dots from 10.004% to 10.425%.

1. Introduction

A recent forecast predicts that photovoltaics will contribute nearly a third of new electricity generation capacity globally between now and 2030. This is due to recent significant reductions in manufacturing costs of mainstream solar cell technology [1]. On all fronts, a new generation of hybrid organic-inorganic halide perovskites provides enticing possibilities [2]. The lead has been a significant component of all highly effective perovskite cells to date, raising toxicity concerns throughout device production, deployment, and disposal, is one drawback of perovskites. Additionally, they typically degrade when exposed to moisture and ultraviolet light, sometimes rather quickly.

Perovskites have many advantageous properties that make them suitable as materials for photons in solar devices. Importantly, it is possible to install the perovskite layer using inexpensive coating and printing methods, indicating that improvements gained for polymer solar cells would apply to this new material system. In fact,

there are reliable fabrication methods for perovskites [1]. Perovskite absorbers have a good absorption coefficient over a large wavelength range [3]. Due to a significant variety of applications, including electrochromic, photovoltaic, and microelectronic devices, TiO_2 thin films have attracted a lot of interest [4]. TiO_2 has a wide energy bandgap, which means it has a good ability to separate electrical charges. This enhances the efficiency of electron transfer from perovskite to TiO_2 and reduces charge loss. It has high chemical stability, which means it can withstand the harsh operating conditions of perovskite solar cells, such as exposure to humidity and high heat. TiO_2 is available in large quantities, and its cost is reasonable compared to other materials used in perovskite solar cells [5, 6]. Zirconium dioxide (ZrO_2) is used as a hole transport layer (HTL) in perovskite solar cells because it is a material that has a suitable energy level that allows the holes to be transferred effectively from the perovskite layer to ZrO_2 . ZrO_2 has the ability to form a good interface with the perovskite layer, which contributes to improved gap transport and reduced charge loss. It has a low refractive index, which helps reduce light loss when passing it through the different layers in the solar cell and increases absorption efficiency [7, 8].

A single layer of atoms bound in a two-dimensional crystalline structure makes up the nanocomposite material known as graphene (G). In terms of transmitting charges, graphene offers a number of unique characteristics. Given its extraordinary capacity for efficiently transferring electrical charges, it is regarded as one of the most well-known electrical conductors. It also has excellent thermal conductivity, which means it can transfer heat very effectively. It has an exceptional ability to withstand high electrical current without losing its efficiency in transporting charges [9].

This study aims to prepare nanocomposites TiO_2/G and ZrO_2/G in the form of thin films by the hydrothermal method as electron and hole transport layers, as well as to prepare perovskite CsPbBr_3 and $\text{CsPbBr}_3\text{QDs}$ as effective materials in the manufacture of solar cells from inorganic perovskites as follows: (FTO/ $\text{TiO}_2\text{-G}/\text{CsPbBr}_3/\text{ZrO}_2\text{-G}/\text{Pt}$) represents the first perovskite solar cell (PSC1) and (FTO/ $\text{TiO}_2\text{-G}/\text{CsPbBr}_3\text{QDs}/\text{ZrO}_2\text{-G}/\text{Pt}$) represents the second perovskite solar cell (PSC2).

2. Materials and Methods

2.1. Preparation of TiO_2/G Thin Film as ETL

Using the drop casting method, a paste made of TiO_2/G nanoparticles was created and evenly distributed over an FTO substrate. 1 g of TiO_2 was combined with 0.03 g of graphene in 5 ml of ethanol, followed by 40 ml of deionized water, and cooked hydrothermally for 72 h at 180°C in an autoclave. The autoclave was cooled to room temperature following the reaction. To create the nanocomposite TiO_2/G powder, the precipitate was filtered, repeatedly washed with distilled water and ethanol, and then overnight dried at 50°C . The TiO_2/G nanocomposite was combined with 5 ml of ethanol to make the TiO_2/G paste. The mixture was then stirred with a magnetic stirrer for 48 h at room temperature while 0.25 g of ethyl cellulose and 0.1 cc of citric acid were added. TiO_2/G film is produced using the drop casting method by drizzling a solution droplet onto the FTO glass with an effective area of 2 cm^2 , and the film is then allowed to dry at room temperature. These as-fabricated TiO_2/G films ETL are then annealed at 450°C for better film-to-FTO adhesion (See Figure.1).



Figure (1). The scheme of preparation TiO_2/G as ETL thin film preparation by doctor blade method.

2.2. Synthesis of ZrO₂/G Nanocomposite as HTL

To make ZrO₂/G Nanocomposite, 50 ml of distilled water was mixed with 0.5 g of graphene and 25 g of ZrO₂, and after 5 h of ultrasonication, the suspension was placed into a 100 ml Teflon-lined stainless-steel autoclave. Following that, the autoclave was maintained for 10 h at a preset temperature of 180°C. The dark product was rinsed many times with distilled water after reaching room temperature. Then, ZrO₂/G was filtered out and dried in a vacuum for 12 h at 80°C.

2.3. Synthesis of CsPbBr₃ and CsPbBr₃ QDs Thin Films

We used a pipette to add 5 ml of DMF: DMSO (4:6) to 1.835 g of PbBr₂ to create a 1M PbBr₂ solution. We then sealed the bottle with sealing tape and set it on the magnetic stirrer at 100 °C with continuous stirring until the white powder was entirely dissolved. We next made a 0.07M CsBr solution (1.491 g of CsBr) and added methanol before transferring the beaker to the ultrasonic apparatus to dissolve the white powder entirely. To make perovskite films, the TiO₂/G layer was treated with drops of PbBr₂ solution at 2000 rpm for 40 s, dried at 80 °C for 30 min, and then treated with drops of CsBr solution at 2000 rpm for 40 s. For five minutes, the film was heated to 250 °C. A perovskite-based CsPbBr₃ film was created by carrying out the CsBr deposition four times. As for the synthesis of CsPbBr₃ QDs, we followed the same methods used by Taolin et al [10]. We added 0.18 g of PbBr₂ and 0.10 g of CsBr to 10 ml of N, N-dimethylformamide (DMF). The mixture was transferred to a 150 ml beaker until the solid powder dissolved completely. At room temperature, a magnetic stirrer was used to stir the liquid. Continuous for 5 h. Next, we added 0.5 ml of oleic acid (OA) surfactant and 0.5 mL of oleylamine (OAm). Then 10 ml of the ethyl acetate solution was transferred to a 100 ml beaker. After mixing the solution well, 1 ml was withdrawn and then quickly injected into the ethyl acetate solution. The transparent solution immediately took on a yellow-green color, and this color indicates the formation of the CsPbBr₃ QDs solution. To purify and clean the QDs, the solution was extracted using a centrifuge for 3 min. After decanting the supernatant, the precipitate was suspended in an n-hexane solution for storage (See Figure 2).

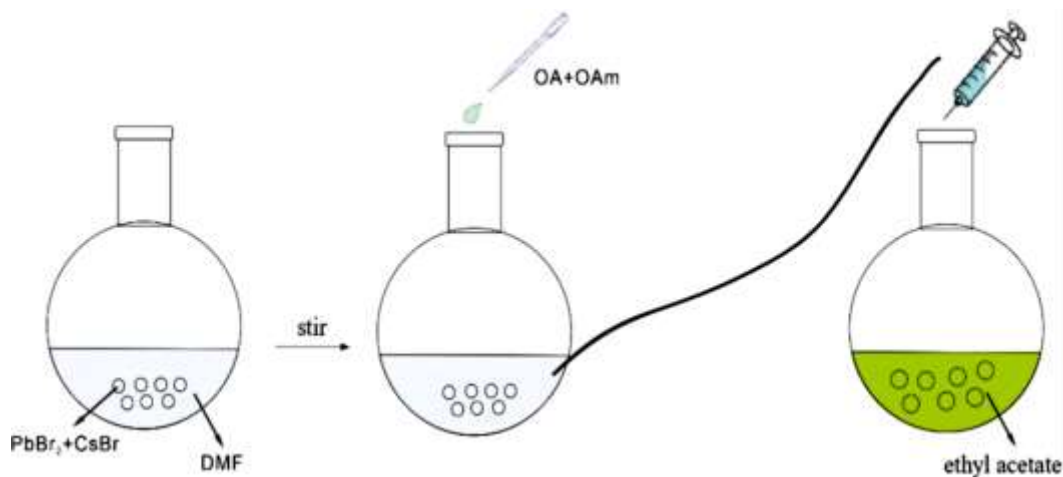


Figure (2). Schematic of synthesis of CsPbBr₃ QDs.

2.4. Fabrication of Devices

We deposited droplets of perovskite CsPbBr₃ on the electrons transport layer (TiO₂/G thin film) by two-step spin coating, after which the substrate was annealed at 250 °C for 30 min, then deposited droplets of ZrO₂/G solution applied as holes transport layer (HTL). Using a spin-coating method the substrate was annealed at 100 °C. Then, the counter electrode (CE) is prepared using TEV technology. By placing a Platinum (pt) wire at a pressure of (10⁻⁵ Torr) and with a surface area of the CE film of (2 cm²) to make (PSC1). Figure (3) shows the structure of the manufactured solar cell. The perovskite layer was replaced by a perovskite QDs layer to form (PSC2).

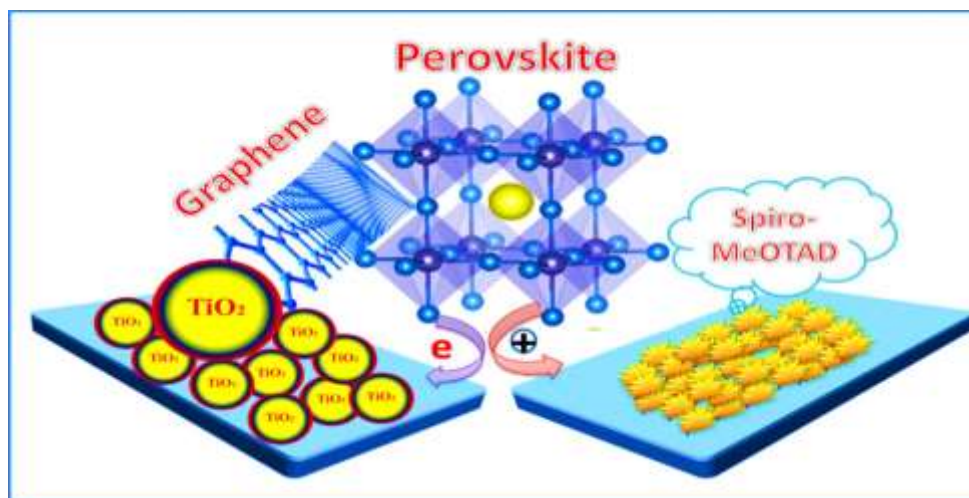


Figure (3). Diagram showing Perovskite Solar Cell structure.

3. Results and Discussion

3.1. X-Ray Diffraction

TiO₂/G thin films' XRD diffraction patterns are displayed in Figure (4a). The findings and the references [11, 12] are in good agreement. Since every diffraction peak has an index, they all coincide with the typical peaks (JCPDS NO. 21-1272). The TiO₂/G thin film has a polycrystalline anatase structure [13] in the X-ray spectrum, which may be directly attributable to the presence of rutile TiO₂ (JCPDS Card No. 21-1276) and contains seven peaks in the diffraction and (211) plane. The (101) direction is where the X-ray's peak is located. The addition of graphene to TiO₂ does not alter the final crystalline structure, according to the XRD data. Although the graphene peak at $2\theta = 26.5^\circ$ may have been covered by TiO₂ nanoparticles, this may be because the strong peak at $2\theta = 25.3^\circ$, which is attributed to the anatase phase of TiO₂, often masks the graphene peak in TiO₂/G nanocomposites. The crystallite size values of TiO₂/G films were estimated using FWHM and 2θ of the directions' peaks using the Debye-Scherrer equation.

Figure (4b) exhibits crystalline diffraction peaks that closely resemble the standard peaks (JCPDS NO. (37-1484) and (41-0017)) and can be used to analyze the crystalline phase of the ZrO₂/G nanocomposite. The graphene nanosheets' XRD pattern shows a peak at $2\theta = 26.48^\circ$ [14, 15]. The cubic structure is indexed to each and every diffraction peak. Debye Scherrer's equation (Eq.1) is used to determine crystallite size. The dimension of nanostructures determined from the TEM results accords with the average crystallite size of 43 nm.

$$D = K\lambda / \beta \cos\theta \quad (1)$$

The X-ray diffraction pattern of the CsPbBr₃ and CsPbBr₃ QDs thin films, respectively, is shown in Figure (4c, d). The experimental peaks are consistent with earlier published literature [16, 17] and closely resemble the conventional CsPbBr₃ peaks (JCPDS file No. 054-0752). The cubic phase in the space was indexed to each peak ($a = b = c = 5.83 \text{ \AA}$). The film showed a significant amount of crystallinity. The CsPbBr₃ QDs XRD pattern then showed strong, identifiable peaks. The XRD patterns of all the perovskite QDs are comparable and nicely crystallized in the cubic phase. The findings were in good accord with those reported by [18]. At 30.7° , the (200) plane's diffraction was quite strong. Its appearance suggested a highly crystalline, pure, and defect-free cubic phase, together with the secondary diffraction peak of the (100) plane. PbBr₂ or CsBr precursor peaks were absent from the pattern. Cs ions occupy the cube's vertices in the space group's cubic symmetry, while Pb and Br ions make up the octahedral {PbBr₆}₄ building blocks. We note that the quantum dot example has a smaller crystal size.

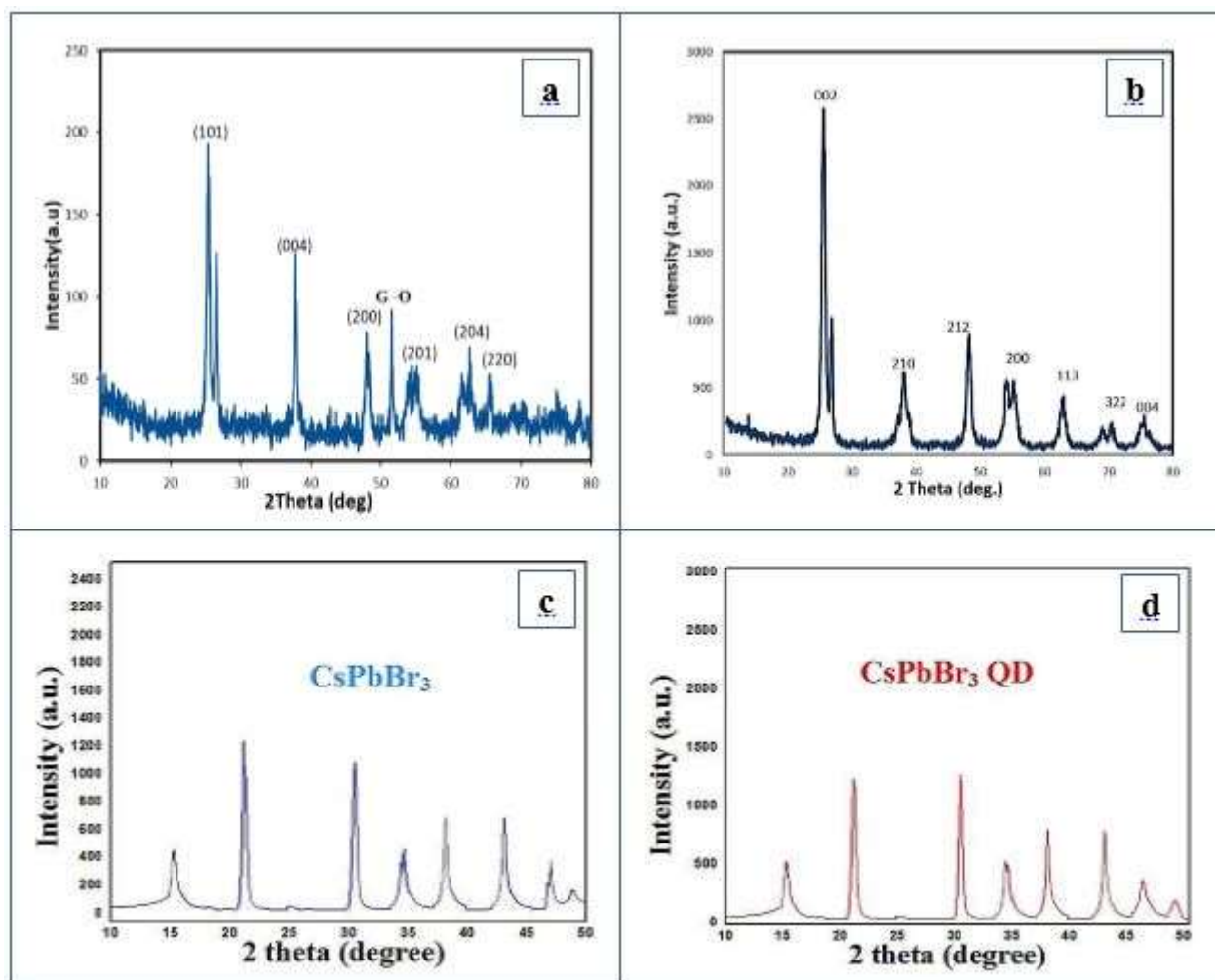


Figure (4). XRD spectra of (a) TiO₂/G film, (b) ZrO₂/G film, (c) CsPbBr₃, and (d) CsPbBr₃ QDs perovskite.

3.2. Morphological Properties

Figure (5) shows the TEM images of the prepared TiO₂/G nanocomposite, this image showed that the nanoparticles were quasi-spherical or spherical aggregates with an average TiO₂/G particle size of about 40–50 nm. Graphene is characterized by its unique chemical composition, which is a thin layer of carbon that consists of carbon atoms arranged in a specific geometric pattern. TiO₂ contains titanium and oxygen atoms bonded in a specific way. Because there is chemical compatibility between the structure of graphene and TiO₂, it contributes to achieving homogeneity and good bonding between them. Because graphene has high bond strength, great flexibility, and good thermal and electrical conductivity. These properties enhance graphene ability to interact and bond with other compounds such as TiO₂ at the nanoscale interface. Since graphene is very thin and consists of only one layer of carbon atoms, it increases the interaction area with TiO₂. This enhances the potential for chemical interaction and bonding between molecules and leads to reliable homogeneity at the nano-level. These factors contribute to achieving strong and stable bonding between molecules and forming a homogeneous nanostructure that is effective in various performances and applications. This may lead to increased current density (J_{sc}) and improved cell power conversion efficiency (PCE).

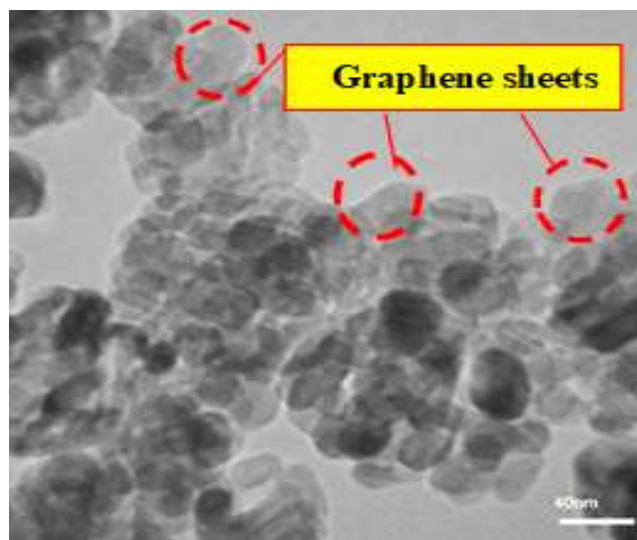


Figure (5). TEM images for TiO₂/G Nanocomposite.

The TEM image shows the homogeneity of ZrO₂/G as a nanocomposite in Figure (6). The microscopic images confirm the formation of well-defined spherical nanoparticles with different sizes from 20–40 nm. The homogeneity of ZrO₂ with graphene as a nanolayer in perovskite solar cells is considered a promising option to improve cell performance and increase its efficiency because graphene is an electrical conductive material, and therefore it can be used as a nanolayer to conduct charge in a perovskite cell. The efficiency of solar energy conversion is increased by the graphene because it enhances charge conduction from the perovskite layer to the counter electrode (pt). Due to ZrO₂ excellent oxidation resistance, corrosion, and long-term performance deterioration are prevented in graphene as a nanostructure. The solar cell's stability and longevity are both improved by doing this. By enhancing charge conduction, decreasing charge loss, and enhancing the absorption rate, all of these characteristics help the cell become more effective and function better.

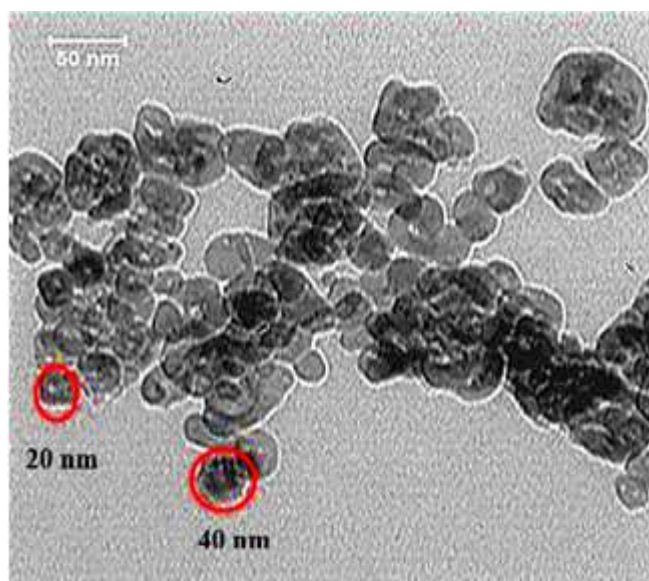


Figure (6). TEM images for ZrO₂/G Nanocomposite.

The SEM image shows the homogeneous distribution of CsPbBr₃ quantum dots and we observe the presence of consistent small particles on the surface of the sample. Quantum dots are composed of (Cs), (Pb) and (Br) ions, and are characterized by their small size that can be clearly seen using an SEM. We also note that quantum dots are regular in size and shape, and can be homogeneous. The CsPbBr₃ nanocomposite is expected to be

homogeneous in composition. Coordinated and homogeneous quantum dots consisting of the component elements of the compound (cesium, lead and bromine) can be seen on the surface of the sample (See Figure 7).

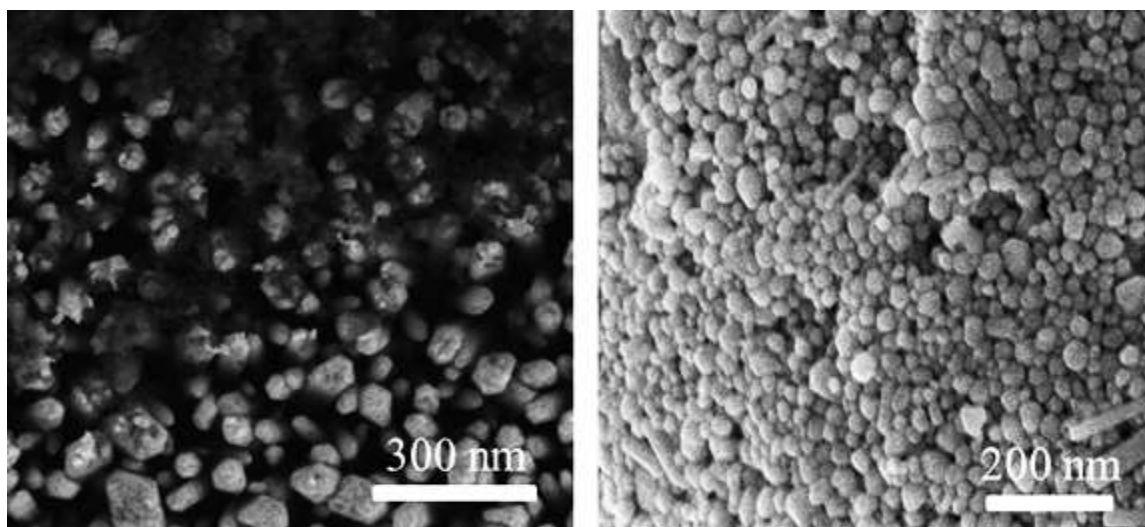


Figure (7). The SEM images for CsPbBr₃ quantum dot

3.3. Optical Properties of CsPbBr₃ and CsPbBr₃ QDs

Figure (8) shows the absorption spectra of the CsPbBr₃ and CsPbBr₃ QDs. quantum dots are small aggregates of nanocomposite atoms. This small size leads to remarkable quantum effects, including increased efficiency of absorption of light at a specific wavelength. Quantum dots have a very high surface-to-volume ratio as a result of their small size and two-dimensional shape. This leads to increased interactions with light and improved absorption efficiency, as there are more opportunities for photons to interact with quantum dots on their surface. Although these factors play an important role in increasing the absorption of light by CsPbBr₃ nanocomposite quantum dots, it should be noted that the precise explanation of these phenomena is complex and still requires further study and research.

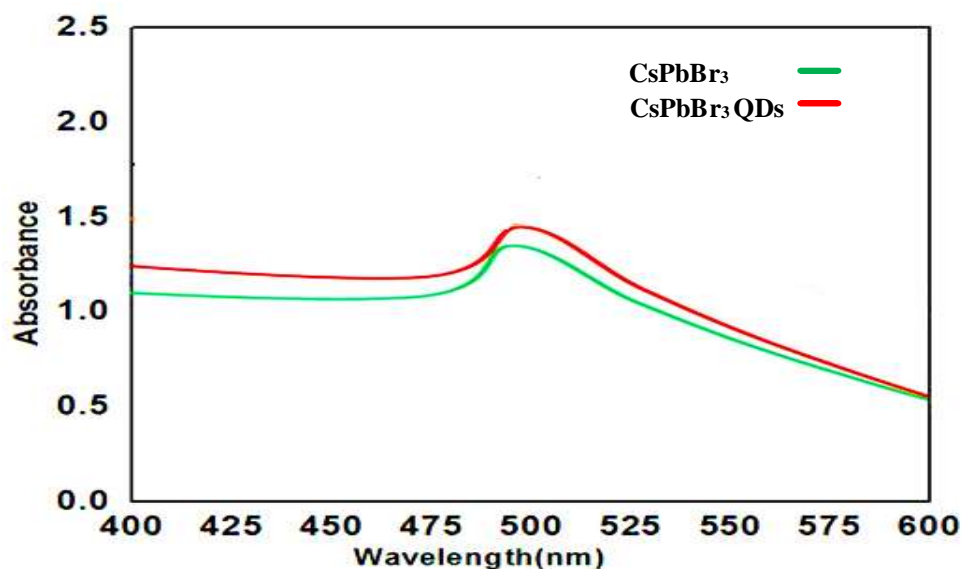


Figure (8). Absorption spectrum of CsPbBr₃, CsPbBr₃ QDs.

3.4. The Photovoltaic Performance

From Figure (9) and Table (1) we notice that the J_{sc} value for the cell (PSC1) has increased compared to the solar cell (PSC2) (from 8.30 to 8.42 $\text{mA}\cdot\text{cm}^{-2}$) as well as in V_{oc} values (from 1.47 to 1.51 V), respectively. This increase leads to an increase in the energy conversion efficiency from 10.004% to 10.425% when using quantum dots of the CsPbBr_3 nanocomposite in the perovskite solar cell. This means that the CsPbBr_3 nanocomposite quantum dots can more efficiently absorb light in the visible and near-visible range which is important for solar power generation. The quantum dots of the CsPbBr_3 nanocomposite interact better with light and increase the chances of absorbing it, which contributes to increasing the efficiency of converting light into electrical energy in the perovskite solar cell. These features can contribute to increasing the energy conversion efficiency of the perovskite solar cell when using CsPbBr_3 nanocomposite quantum dots.

Table (1). Photovoltaic Parameters of perovskite solar cells.

Device	J_{sc} ($\text{mA}\cdot\text{cm}^{-2}$)	V_{oc} (V)	FF	PCE (%)
PSC 1	8.30	1.47	0.82	10.004
PSC 2	8.42	1.51	0.82	10.425

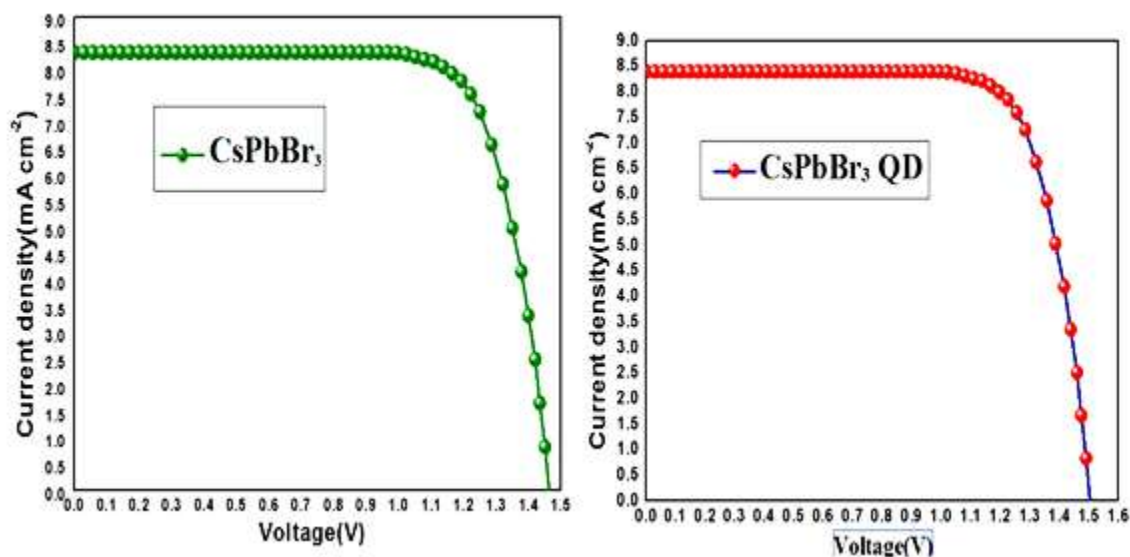


Figure (9). Performance of all perovskite Solar Cells.

4. Conclusions

In conclusion, we manufactured two solar cells and comparing the results improved the optoelectronic properties of CsPbBr_3 by converting it into CsPbBr_3 QDs as the photoactive layer active material in perovskite solar cells. The fabricated device reached the highest power conversion efficiency of 10.425%, which is 10.004% higher than the original device based on CsPbBr_3 as the active material in the photonic layer. Our study included a comprehensive understanding of the use of TiO_2/G as the electron transport layer and ZrO_2/G as the hole transport layer.

Conflict of Interest: The authors declare that there are no conflicts of interest associated with this research project. We have no financial or personal relationships that could potentially bias our work or influence the interpretation of the results.

References

- [1] M. A. Green, A. Ho-Baillie, and H. J. Snaith, "The emergence of perovskite solar cells," *Nat. Photonics*, vol. 8, no. 7, pp. 506–514, 2014.
- [2] N.-G. Park, "Organometal perovskite light absorbers toward a 20% efficiency low-cost solid-state mesoscopic solar cell," *J. Phys. Chem. Lett.*, vol. 4, no. 15, pp. 2423–2429, 2013.
- [3] S. De Wolf *et al.*, "Organometallic halide perovskites: sharp optical absorption edge and its relation to photovoltaic performance," *J. Phys. Chem. Lett.*, vol. 5, no. 6, pp. 1035–1039, 2014.
- [4] P. Bonhôte, E. Gogniat, M. Grätzel, and P. V Ashrit, "Novel electrochromic devices based on complementary nanocrystalline TiO₂ and WO₃ thin films," *Thin Solid Films*, vol. 350, no. 1–2, pp. 269–275, 1999.
- [5] H. S. Jung and N. Park, "Perovskite solar cells: from materials to devices," *small*, vol. 11, no. 1, pp. 10–25, 2015.
- [6] X. Chen and S. S. Mao, "Titanium dioxide nanomaterials: synthesis, properties, modifications, and applications," *Chem. Rev.*, vol. 107, no. 7, pp. 2891–2959, 2007.
- [7] D. Zhang and F. Zeng, "Structural, photochemical and photocatalytic properties of zirconium oxide doped TiO₂ nanocrystallites," *Appl. Surf. Sci.*, vol. 257, no. 3, pp. 867–871, 2010.
- [8] L. Kumari *et al.*, "Controlled hydrothermal synthesis of zirconium oxide nanostructures and their optical properties," *Cryst. Growth Des.*, vol. 9, no. 9, pp. 3874–3880, 2009.
- [9] J. H. Warner, F. Schaffel, M. Rummeli, and A. Bachmatiuk, *Graphene: Fundamentals and emergent applications*. Newnes, 2012.
- [10] T. Ma, J. Wang, J. Qian, S. Ye, Y. Zhou, and Y. Wang, "Synthesis and optimization of cesium lead halide perovskite QDs," *Appl. Phys. A*, vol. 127, pp. 1–7, 2021.
- [11] A. Tayel, A. R. Ramadan, and O. A. El Seoud, "Titanium dioxide/graphene and titanium dioxide/graphene oxide nanocomposites: Synthesis, characterization and photocatalytic applications for water decontamination," *Catalysts*, vol. 8, no. 11, p. 491, 2018.
- [12] R. H. Sakban, S. M. Abdulmohsin, and M. D. Noori, "Glucose Bio Sensor Base Nanocomposite Graphene/TiO₂," in *Journal of Physics: Conference Series*, 2021, vol. 1818, no. 1, p. 12038.
- [13] R. Belchi *et al.*, "One-step synthesis of TiO₂/graphene nanocomposites by laser pyrolysis with well-controlled properties and application in perovskite solar cells," *ACS omega*, vol. 4, no. 7, pp. 11906–11913, 2019.
- [14] R. S. Das, S. K. Warkhade, A. Kumar, and A. V Wankhade, "Graphene oxide-based zirconium oxide nanocomposite for enhanced visible light-driven photocatalytic activity," *Res. Chem. Intermed.*, vol. 45, pp. 1689–1705, 2019.
- [15] N. C. Horti, M. D. Kamatagi, S. K. Nataraj, M. N. Wari, and S. R. Inamdar, "Structural and optical properties of zirconium oxide (ZrO₂) nanoparticles: effect of calcination temperature," *Nano Express*, vol. 1, no. 1, p. 10022, 2020.
- [16] M. Zhao, Y. Shi, J. Dai, and J. Lian, "Ellipsometric study of the complex optical constants of a CsPbBr₃ perovskite thin film," *J. Mater. Chem. C*, vol. 6, no. 39, pp. 10450–10455, 2018.
- [17] W. Zhihai *et al.*, "Air-stable all-inorganic perovskite quantum dot inks for multicolor patterns and white LEDs," *J. Mater. Sci.*, vol. 54, pp. 6917–6929, 2019.
- [18] S. M. H. Qaid, H. M. Ghathani, B. A. Al-Asbahi, A. Alqasem, and A. S. Aldwayyan, "Fabrication of thin films from powdered cesium lead bromide (CsPbBr₃) perovskite quantum dots for coherent green light emission," *ACS omega*, vol. 5, no. 46, pp. 30111–30122, 2020.